Probabilistic reconstruction (or forecasting) of distal runouts of large magnitude ignimbrite PDC flows sensitive to topography using mass-dependent inversion models.

ISTITUTO NAZIONALE DI GEOFISICA E VULCANOLOGIA

University of BRISTOL

WEST JEC 西日本技術開発株式会社

AGU 100 FALL MEETING San Francisco, CA | 9–13 December 2019

Paper Number NH21D - 0997
Abstract ID: 575290

Willy Aspinall(1), **Andrea Bevilacqua**(2), Antonio Costa(2), Hirohito Inakura(3), Sue Mahony(1), Augusto Neri(2), Stephen Sparks(1).

(1) University of Bristol, School of Earth Sciences, Bristol, United Kingdom, (2) Istituto Nazionale di Geofisica e Vulcanologia, Sezione di Pisa, Pisa, Italy, (3) West Japan Engineering Consultants, Inc., Fukuoka, Japan.

1. A method to model the minimum volume and mass to inundate an at-risk city from a volcano source site

Our analysis relies on the implementation of several versions of the integral formulation for **axisymmetric gravity-driven particle currents**, based on the pioneering work of Huppert and Simpson (1980). The theory is detailed in Bonnecaze et al., (1995) and Hallworth et al. (1998). We focus on models which possess analytical solutions, enabling us to utilise a very **fast functional approach** in the uncertainty quantification process. Further details on the **physical equations** we adopted, as well as the expression of **analytical solutions**, can be found in Biagioli et al., 2019.

In particular, we focus on two different models:

- **Model 1** – [Rock avalanche dynamics with constant stress over the flow basal area]
  This model for energy dissipation is described in Dade and Huppert (1998). It assumes the entire amount of solid material **falls from a prescribed height**. Constant stress dynamics has been further explored in Kelfoun et al. (2009); Kelfoun (2011).

  INPUT parameters:
  H - Collapse Height
  rho_c - Flow density
  tau – equivalent stress*
  *one third of the constant stress value

- **Model 2** – [Density current dynamics with particle deposition and buoyancy effects]
  This model is described in Dade and Huppert, 1995. It has been developed for the simulation of oceanic turbidity currents and then adapted to the simulation of **large-scale ignimbrites** (Dade and Huppert, 1996).

  INPUT parameters:
  phi0 – initial solid fraction
  ws – velocity of settling of the solid particles
  rho – density of solid particles
  rho_a – density of ambient air
  rho_i – density of interstitial gas

In our implementation, Model 2 assumes **monodispersed solid particles**, because the modelling of the full Total Grain Size Distribution (TGSD) does not produce analytical solutions. The Sauter diameter is believed to provide a reasonable approximation to the dynamics of the full TGSD.
We assume a fixed volume **instantaneous release** of collapsing material, as in Neri et al. (2015); Bevilacqua (2016); Esposti Ongaro et al. (2016); Bevilacqua et al. (2017), Biagioli et al., (2019).

We present three variants of Model 2:

- **Model 2a.** This variant includes **interstitial gas, thermally buoyant** with respect to surrounding cold air. The flow stops propagating when the solid fraction *phi(t)* becomes lower than a critical value *phi_cr*, and the remaining mixture of gas and particles lifts off, possibly generating a phoenix cloud.
- **Model 2b.** The modelling equations in this variant are equivalent to the previous model, but an alternative input of *ws* is adopted, expressed as a range of values. This range is based on the law of particle terminal velocity (Armienti et al., (1988); Bonadonna and Phillips, (2003); Dioguardi et al., (2017)) at the scale of the Sauter diameter for ***analogue flows***. These flows are: Mt St. Helens (Costa et al., 2016), Campanian Ignimbrite (Costa et al., 2012; Marti et al., 2016), Youngest Toba Tuff (Costa et al., 2014). Moreover, this variant implements an alternative input range of *phi0*, based on MDR modeling (Costa et al., 2018).
- **Model 2c.** This variant assumes an interstitial gas equivalent to **ambient air**. Thermal buoyancy effects are absent, and the flow stops when *phi(t)*=0.

Model 2 assumes **thermal properties remain constant** for the duration of the flow. Thermodynamics modelling of cooling effects (e.g. Bursik and Woods, 1996; Fauria et al., 2016) could be further explored in follow up research.

2. Input ranges based on Expert Judgment

We based our input range estimation on **structured expert judgment** (Cooke, 1991; Aspinall, 2006). For judgment aggregation, we implemented the **equal weight combination rule**; we did not apply performance-based scores because of the relatively small number of experts participating and because the overheads and time demands involved in implementing a formal elicitation protocol were not warranted in this case.

Reported values express the **percentiles of the probability distribution** obtained by pooling experts' judgments (also called the solution Decision Maker DM).

We assumed the inputs to be formed of an array of independent variables.
Further research may explore the effects of possible correlations between them.

Elicitation solution #1

Case name: Model 1 08/01/2019

Resulting solution (joint DM distribution of values assessed by experts)

Nr.	Id	Scale	5%	50%	95%	Units
1	Collapse *H*	uni	2566	5752	9629	m
2	Flow density	uni	686.3	992	1511	kg/m^3
3	Stress	uni	244.3	1868	7666	Pa
4	Lambda+	uni	1.945	3.044	3.142	rad

+in the sequel lambda will be fixed to pi unless otherwise stated.

Elicitation solution #2

Case name: Model 2 02/02/2019

Resulting solution (joint DM distribution of values assessed by experts)

Nr.	Id	Scale	5%	50%	95%	Units
1	*phi0*	uni	0.001789	0.01103	0.03675	
2	Ws	uni	0.04492	0.4405	2.460	m/s
3	*rho*	uni	1089	1814	2357	kg/m^3
4	*rho_a*	uni	1.023	1.193	1.284	kg/m^3
5	*rho_i*	uni	0.3184	0.4853	0.7957	kg/m^3

2.1 Energy cone inference as "Model 0"

Before running the models described above, we used the elicited Collapse Height *H* to calculate the Minimum Volume (*MinVol*) required to reach 130 km runout, according to the **Energy Cone linear regression** in Ogburn and Calder (2017).

Minimum PDC Volume [km³]				
1%ile	5%ile	50%ile	mean	95%ile
13.4	16.9	669	1.92×10^5	4.1×10^5

The minimum volume (MinVol) estimates reported here appear to capture the same order of magnitude as results in the other models in terms of the lower percentile values. However, the mean and 95th percentile of MinVol look **infeasibly large**, numerically; Model 0 will not be considered when compiling a combination of the models.

Modified input range based on MDR modelling and Sauter diameter of analogues

Nr.	Id	Scale	MIN	MAX	Units
1*	*phi0*	uni	0.002	0.01	
2*	*ws*	uni	0.04	0.3	m/s

*these results approximately impose input values in the range [min, median] assessed by joint DM.

3. Output ranges Minimum PDC Volume and Equivalent Mass

The following results represent the required volume necessary to inundate an **at-risk city at 130 km** from the source of the flow, i.e. an hypothetical volcano.
The value of the P^{th} percentile is the volume amount that has probability P to inundate the at-risk city, according to the **probability distribution of the model inputs**.

Bayes Net calculation results, using Volume

Model	Maximum distance 130 km	Minimum PDC Volume [km³]				
		1%ile	5%ile	50%ile	mean	95%ile
D&H98	(1) Elicited inputs	11.5	26.0	263	450	1474
D&H95 w/hot gas	(2a) Elicited inputs	5.68	10.2	55.9	77.9	226
	(2b) Modified inputs*	5.35	7.30	16.7	17.4	30.0
D&H95	(2c) Elicited inputs	3.34	6.80	43.5	64.5	201

*modified *phi0* and *ws* based on MDR modelling and Sauter diameter of analogues.

To obtain a consistent comparison of the two models requires the calculation of **equivalent mass**, because the **model volumes have a different meaning**.

In particular:
Model 1, based on Dade and Huppert (1998), **does not include gas**.
The volume calculated represents the bulk solid material, at a density of about 1000 kg/m³ (deposit).

Model 2, based on Dade and Huppert (1995), is **multi-phase and includes solid particles and interstitial gas**.
As a model option, this gas can be assumed hot and buoyant with respect to ambient air.
The volume calculated only represents the solid phase, at a density of about 2300 kg/m³ (rhyolite, Bonadonna et al., 2003).

Optional corrections of these values can include:
- Site shielding effects of local topography: *MinVol* +104%
- Asymmetries in the flow propagation: *MinVol* -15%.

Bayes Net calculation results, using Equivalent Mass

Model	Maximum distance 130 km	Minimum PDC Mass [10^{12} kg]				
		1%ile	5%ile	50%ile	mean	95%ile
D&H98	(1) Elicited inputs	11.5	26.0	263	450	1474
D&H95 w/hot gas	(2a) Elicited inputs	13.1	23.5	129	179	520
	(2b) Modified inputs*	12.3	16.8	40.7	40.0	69.0
D&H95	(2c) Elicited inputs	7.68	15.6	100	148	462

Model 2 is reported in **three variants**:

- Model 2a includes hot gas effects, and relies on the **elicited input ranges** of phi0, ws, rho, rho_a, rho_i.
- Model 2b includes hot gas effects, and relies on modified **input ranges based on MDR modelling** and Sauter diameter of analogues. These results impose lower phi0 and ws values than in the previous case.
- Model 2c **does not include hot gas** effects, and relies on the elicited input ranges of phi0, ws, rho, rho_a.

Through a Monte Carlo simulation randomly sampling the models, we also averaged the **four probability distributions** obtained. We assigned equal weights to the four modelling choices (Model 1, 2a, 2b, 2c). This is equivalent to a linear combination of the models' *pdf* or *cdf* (see Cooke, 1991; Bevilacqua, 2016).

Model Mixture	Minimum PDC Mass [10^{12} kg]				
	1%ile	5%ile	50%ile	mean	95%ile
	10.9	18.4	86.0	204	735

THIS STUDY SPECIFICALLY FOCUSES ON THE **NEW METHOD**.

WE APPLIED THE METHOD IN A **HYPOTHETICAL EXAMPLE** OF MAJOR IGNIMBRITE SCENARIO.

WE USED A NON-EXISTING **TOPOGRAPHY** AND ARBITRARY ERUPTIVE **MASS BOUNDS**.

ANY RELATION TO REAL VOLCANOES OR REAL AT-RISK CITIES IS **PURELY COINCIDENTIAL**.

4. PDC inundation probability at an at-risk city based on eruption size

In **Figure 1** we show the cumulative distribution of **Equivalent Mass** required to reach the at-risk city, according to the **four models** described. We based a first analysis on the Dense Rock Equivalent (DRE) volume of a major ignimbrite eruption, first we assume an example **volume of 200 km³**. We converted this DRE volumes to a mass of $500 \cdot 10^{12}$ kg units), assuming a density of 2500 kg/m³ (DRE rhyolite).

PROBABILITY P OF PDC FLOW REACHING THE AT-RISK CITY, 130 km RUNOUT [VDRE 200km³]

- Combined model - 89.9%
- Model 1 (avalanche *tau*-friction) - 68.9%
- Model 2a (box model with hot gas) - 94.2%
- Model 2b (Sauter-based *ws*, MDR-model-based *phi0*) - 100%
- Model 2c (cold gas) - 96.4%

PROBABILITY P OF PDC FLOW REACHING THE AT-RISK CITY, 170 km RUNOUT [VDRE 200km³, with topo-effects]

- Combined model - 76.0%
- Model 1 (avalanche *tau*-friction) - 48.1%
- Model 2a (box model with hot gas) - 75.1%
- Model 2b (Sauter-based *ws*, MDR-model-based *phi0*) - 100%
- Model 2c (cold gas) - 80.9%

CUMULATIVE DISTRIBUTION OF EQUIVALENT MASS

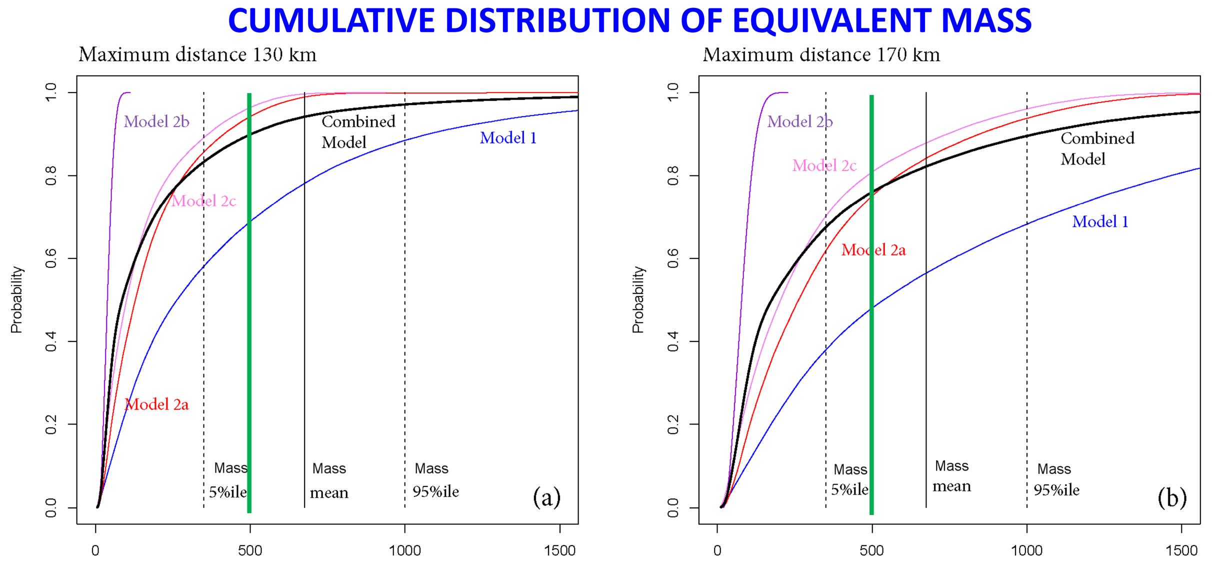

FIGURE 1. **Cumulative distribution** of the minimum mass MassMin variable, representing Equivalent Mass required to reach the at-risk city.

(a) is related to a maximum runout distance of 130 km, i.e. between volcano and at-risk city; (b) is related to a maximum runout distance of 170 km, allowing for the flow to overcome possible topography shielding effects near the site.

The **black bold** line is the combined model, described above. **Blue line** is Model 1, **Red line** is Model 2, **Purple line** is Model 2b, **Pink line** is Model 2c.

A **green** vertical line marks the mass estimate related to the VDRE of 200 km³. **Black** vertical lines mark the mean and uncertainty percentiles of an estimate of plausible erupted mass, i.e. obtained from VDRE [140, 270, 400] km³ .

Fig. 1 also implements more detailed estimates: i.e. [140, 270, 400] km³, 5th, mean, and 95th percentile values respectively. According this **uncertain erupted volume range**, and the combined runout model results, we have inundation probability: ***P* = [67.5%, 82.2%, 89.5%]**

An optional correction for flow direction asymmetries produces the following adjustment: P = [71.6%, 85.4%, 92.1%].

5. Example of the effects of distal and medial topography

The realization of 130 km runout L in absence of topography is **not a sufficient condition** to impact a distant important city and any evacuation decision. We report examples of inundated regions as a function of runout distance L, according to the energy conoid technique.

We follow the **'energy conoid'** approach adopted in Neri et al., (2015) and Bevilacqua et al., (2017). **Figure 2** shows inundation maps based on the comparison of kinetic energy available to the flow and **local topography along radial direction**. Energy calculation is based on the equations of Model 2c, with illustrative values of phi0=1% and rho=2000 kg/m³.

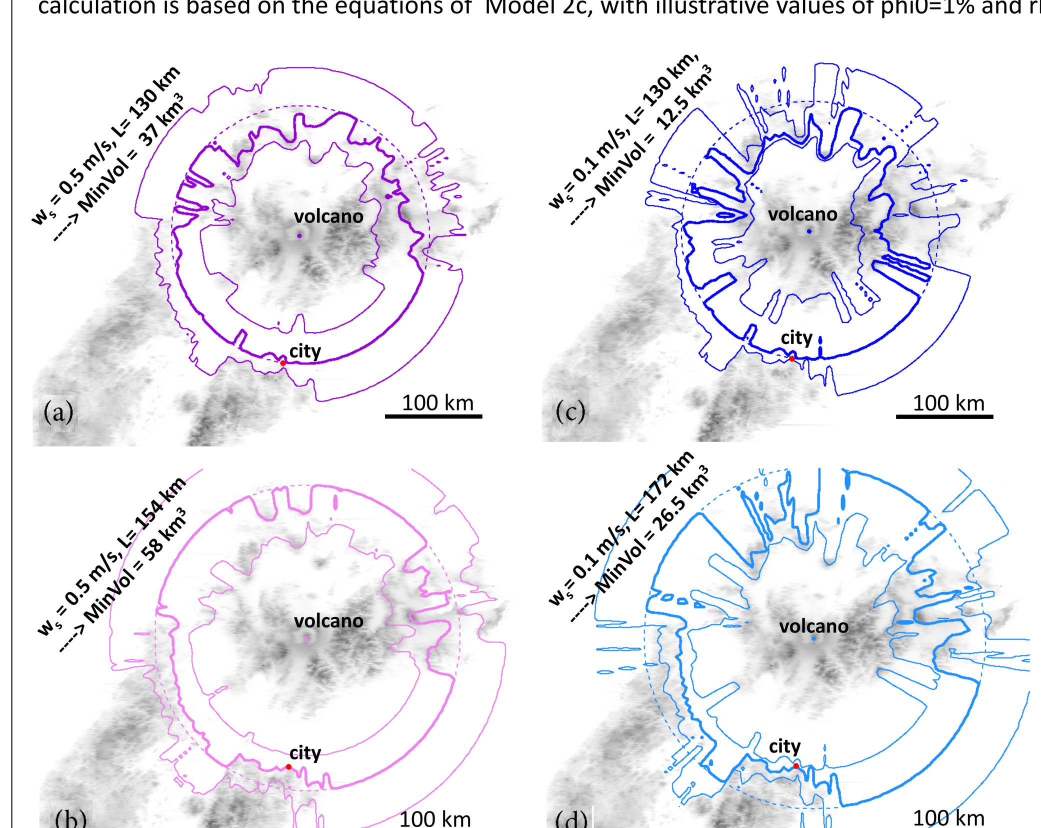

FIGURE 2. Panels (a),(c) show the **inundated region** assuming L=130 km³; (b),(d) show the inundated region assuming the minimum L required to affect the at-risk city considering **shielding effects** of local topography. Shades of black display topographic obstacles (i.e. mountain ranges).

(a),(b) are based on w_s=0.5 m/s, and (c),(d) assume w_s=0.1 m/s. All the pictures assume phi0=1% and rho=2000 kg/m³, and the minimum volume estimate V is displayed.

A coloured dot marks the volcano, and a red dot marks the at-risk city. A bold coloured line marks the **boundary of the inundated** region based on volume V. A thin dashed line marks a circle of radius L. Thin coloured lines mark the boundaries of the inundated region based on V/2 and 2V, for comparison.

Topography, volcano, and at risk city are an hypothetical example.

According to the analytic expression of the ***MinVol* variable**, a more conservative assumption of requiring a runout of 170 km would **double** the required erupted volume in order to inundate the at-risk city.
We remark that our energy conoid approach is only sensitive to the shielding effect of **topography close to the at-risk city**, and not on the large-scale topography around the source site .

6. Sensitivity analysis

We use a **Bayes Belief Network** (BBN) related to each model to characterize uncertainties on the *MinVol* estimate, including in the calculational scheme correlation coefficients between the input variables and the calculated *MinVol* [Ababei (2016); UNINET BBN: https://lighttwist-software.com/ accessed 25 Nov 2019].

The large rectangular panels in each BNN illustrate the shape of the **uncertainty distribution for the minimum volume** needed to reach the at-risk city, based on the uncertainties in the relevant input variables, with the mean value and standard deviation shown in the lower frame of the panel.

Larger **correlation values** (marked on linking arc arrows) highlight the **more sensitive variables**. Negative correlation means that an increase of that input decreases the *MinVol* required to reach the at-risk city. Positive correlations produce the opposite effect.

The correlation coefficients are based on **the joint DM distribution** from elicitation and on the 130 km maximum runout distance. Further research is merited to develop better constraints on the uncertainty distributions of the most **influential input parameters**.

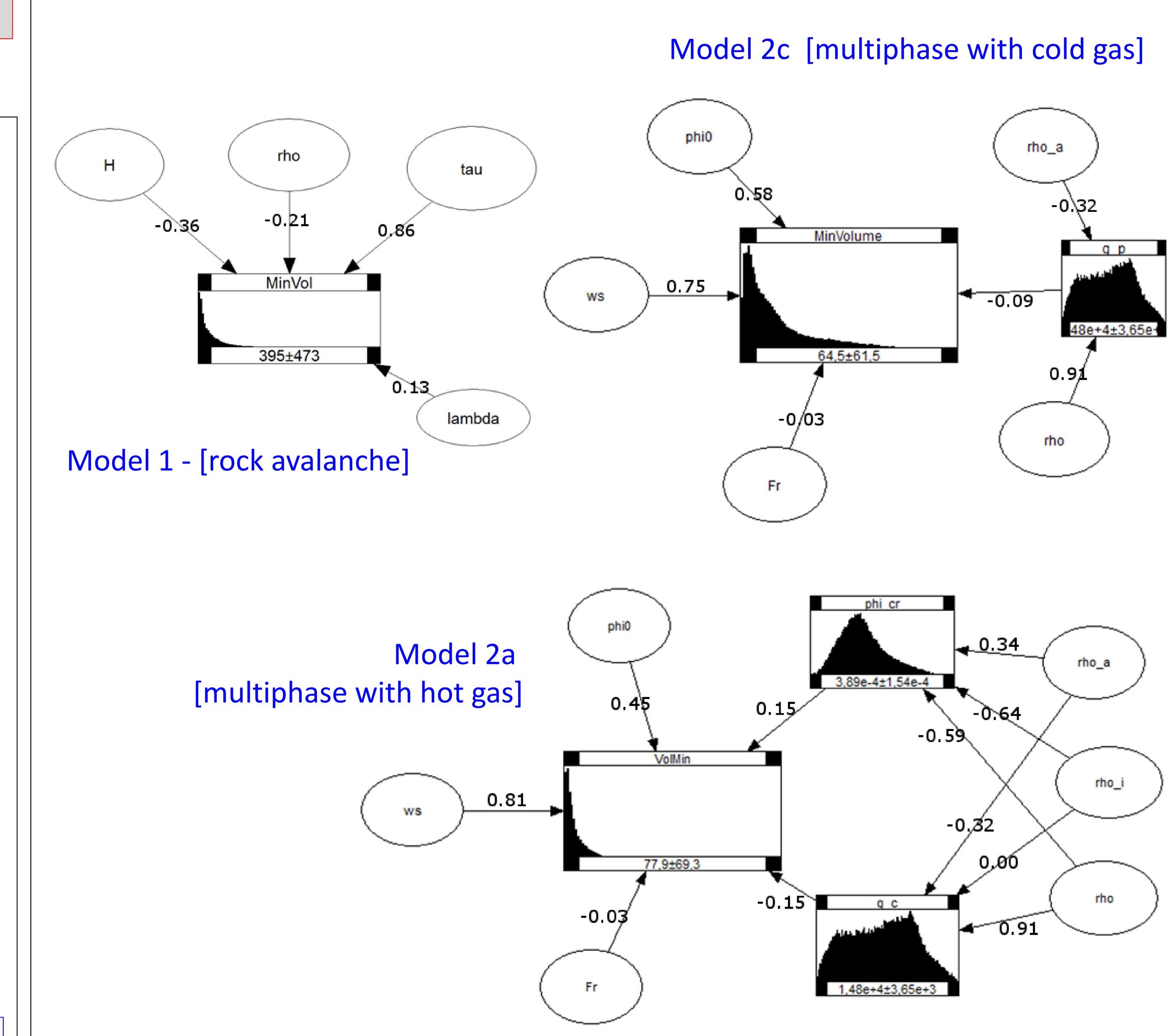

5. Conclusions

We described a new method for the **reconstruction (or forecast)** of probabilities that distal geographic locations were inundated by a giant pyroclastic density current (PDC) in terms of the flow mass and related uncertainties.

Using appropriate model input uncertainty distributions, derived from **expert judgments** using the equal weights combination rule, we estimated the mass amount needed to reach a particular distal locality at any given confidence level and compared this with a range of plausible eruptive masses. in a **hypothetical major ignimbrite scenario**

Our analysis relied on different versions of the Huppert and Simpson (1980) integral formulation of axisymmetric gravity-driven particle currents. We focused on models which possess **analytical solutions**, enabling us to utilize a very fast functional approach for enumerating results and uncertainties.

In particular, we adapted the '**energy conoid**' approach to generate inundation maps along radial directions, based on comparison of the mass-dependent kinetic energy of the flow with the **potential energy control by topography** in the direction of flow at distal ranges.

We focused on two different models:
(i) Model 1 assumes the entire amount of **solid material** originates from a prescribed height above the volcano and flows as a granular current slowed down by **constant friction**;

(ii) Model 2 is a **multi-phase formulation** and includes, in addition to suspended particles, interstitial gas thermally buoyant with respect to surrounding cold air. In the latter case, the flow stops propagating when the solid fraction becomes less than a critical value, and there is **lift-off of the remaining mixture** of gas and small particulates.

Our model parameters can be further constrained where there is reliable field data or with information from analogue eruptions.

Finally, we used a **Bayes Belief Network** related to each inversion model to evaluate probabilistically the uncertainties on the mass required, estimating correlation coefficients between the input variables and the calculated mass.

For any major magnitude ignimbrite PDC scenario, our method provides a rational basis for assessing the **probability of flow inundation** at critical geographic locations within distal areas when there is major uncertainty about the actual or predicted extent of flow runout.

References:

Ababei, D., (2016) UNINET. Software designed by the Risk and Environmental Modeling Group, Delft University of Technology. Lighttwist Software; Fitzroy North, Vic. Australia.
Armienti, P., G. Macedonio, M.T. Pareschi (1988), A numerical model for simulation of tephra transport and deposition applications to May 18, 1980, Mount St. Helens eruption, JGR, 93, B6, 6463-6476.
Aspinall, W. P. (2006), Structured elicitation of expert judgment for probabilistic hazard and risk assessment in volcanic eruptions, in Statistics in Volcanology, Geological Society of London on behalf of IAVCEI, edited by H. M.Mader et al., 296 pp., Geological Society for IAVCEI, London.
Bevilacqua, A. (2016), Doubly stochastic models for volcanic hazard assessment at Campi Flegrei caldera, Theses, 21, Edizioni della Normale, Birkhäuser/Springer, 227p, Pisa, ISBN 978-88-7642-577-6.
Bevilacqua A, A. Neri, M. Bisson, T. Esposti Ongaro, F. Flandoli, R. Isaia, M. Rosi, S. Vitale (2017) The Effects of Vent Location, Event Scale, and Time Forecasts on Pyroclastic Density Current Hazard Maps at Campi Flegrei Caldera (Italy), Front Earth Sci 5:72.
Biagioli, G.,Bevilacqua, A., Esposti Ongaro, T., de' Michieli Vitturi, M. (2019, March 29). PyBox: a Python tool for simulating the kinematics of Pyroclastic density currents with the box-model approach, Reference and User's Guide (Version 0.9). http://doi.org/10.5281/zenodo.2616551
Bonadonna, C., and J. Phillips (2003), Sedimentation from strong volcanic plumes, JGR, 108, B7, 2340-2368.
Bonnecaze, R.T., M.A. Hallworth, H.E. Huppert, J.R. Lister (1995), Axisymmetric particle-driven gravity currents, J Fluid Mechanics, 294, 93-121.
Bursik, M.I., A.W. Woods (1996), The dynamics and thermodynamics of large ash flows, Bull Volcanol, 58, 175-193.
Cooke, R. M. (1991), Experts in Uncertainty: Opinion and Subjective Probability in Science, 336 pp., Oxford Univ. Press, New York.
Costa, A., A. Folch, G. Macedonio, B. Giaccio, R. Isaia, V.C. Smith (2012), Quantifying volcanic ash dispersal and impact of the Campanian Ignimbrite super-eruption, Geophys Res Lett, 39, L10310.
Costa, A., V.C. Smith, G. Macedonio, N.E. Matthews (2014), The magnitude and impact of the Youngest Toba Tuff super-eruption, Front Earth Sci 2:16.
Costa, A., L. Pioli, C. Bonadonna (2016), Assessing tephra total grain-size distribution: Insights from field data analysis, ESPL, 443, 90-107.
Costa, A., Y.J. Suzuki, T. Koyaguchi (2018), Understanding the plume dynamics of explosive super-eruptions, Nature Comm, 9:654.
Dade, W.B., H.E. Huppert (1995), Runout and fine-sediment deposits of axisymmetric turbidity currents, JGR, 100, C9, 18597-18609.
Dade, W.B., H.E. Huppert (1996), Emplacement of the Taupo Ignimbrite by a dilute turbulent flow, Lett Nature, 381, 509-512.
Dade, W.B., H.E. Huppert (1998), Long-runout rockfalls, Geology, 26, 9, 803–806.
Dioguardi, F., D. Mele, P. Dellino (2018), A new one-equation model of fluid drag for irregularly shaped particles valid over a wide range of Reynolds number. JGR, 123, 144– 156.
Esposti Ongaro, T., S. Orsucci, F. Cornolti (2016), A fast, calibrated model for pyroclastic density currents kinematics and hazard, JVGR, 327, 257-272.
Fauria, K. E., M. Manga, and M. Chamberlain (2016), Effect of particle entrainment on the runout of pyroclastic density currents, JGR, 121, 6445–6461.
Hallworth, M.A., A. Hogg, H.E. Huppert (1998), Effects of external flow on compositional and particle gravity currents, J Fluid Mech, 359, 109-142.
Huppert, H.E., J.E. Simpson (1980), The slumping of gravity currents, J Fluid Mech, 99, 4, 785-799.
Kelfoun, K., P. Samaniego, P. Palacios, D. Barba (2009), Testing the suitability of frictional behaviour for pyroclastic flow simulation by comparison with a well-constrained eruption at Tungurahua volcano (Ecuador), Bull Volcanol (2009) 71, 1057.
Kelfoun, K. (2011), Suitability of simple rheological laws for the numerical simulation of dense pyroclastic flows and long-runout volcanic avalanches, JGR, 116, B08209.
Marti, A., A. Folch, A. Costa, S. Engwell (2016), Reconstructing the plinian and coignimbrite sources of large volcanic eruptions: A novel approach for the Campanian Ignimbrite, Sci Rep, 6:21220.
Neri, A., A. Bevilacqua et al. (2015), Quantifying volcanic hazard at Campi Flegrei caldera (Italy) with uncertainty assessment: II. Pyroclastic density current invasion maps, JGR, 120, 2330–2349.
Ogburn, S.E., E.S. Calder (2017), The Relative Effectiveness of Empirical and Physical Models for Simulating the Dense Undercurrent of Pyroclastic Flows under Different Emplacement Conditions, Front Earth Sci 5:83.

Acknowledgements:
This work was supported by Aspinall & Associates. We thank Charles Connor, Laura Connor, Britt Hill and the other experts participating in the elicitation sessions.